NUCL SCI TECH (2017) 28:7
DOI 10.1007/s41365-016-0162-y

Characterization of a broad-energy germanium detector for its use in CJPL

Zhi Zeng[1] · Yu-Hao Mi[1] · Ming Zeng[1] · Hao Ma[1] · Qian Yue[1] · Jian-Ping Cheng[1] · Jun-Li Li[1] · Rui Qiu[1] · Hui Zhang[1]

Received: 10 May 2016 / Revised: 4 July 2016 / Accepted: 29 July 2016 / Published online: 30 November 2016

Abstract The broad-energy germanium (BEGe) detector, with the ability of background discrimination using pulse shape discrimination, is a competitive candidate for neutrinoless double beta decay ($0\nu\beta\beta$) experiments. In this paper, we report our measurements of key parameters for detector modeling in a commercial p-type BEGe detector. Point-like sources are used to investigate energy resolution and linearity of the detector. A cylindrical volume source is used for efficiency calibration. With an assembled device for source positioning and a collimated ^{133}Ba source, the detector is scanned to check its active volume. Using an ^{241}Am point-like source, the dead layer thicknesses is measured at about 0.17 mm on the front and 1.18 mm on the side. The detector characterization is of importance for BEGe detectors to be used in the $0\nu\beta\beta$ experiments at China JinPing underground Laboratory (CJPL).

Keywords BEGe · Characterization · Dead layer · $0\nu\beta\beta$ · CJPL

This work is partly supported by National Natural Science Foundation of China (Nos. 11175099 & 11355001) and Tsinghua University Initiative Scientific Research Program (Nos. 20151080354 & 2014Z21016).

✉ Hao Ma
mahao@tsinghua.edu.cn

[1] Key Laboratory of Particle and Radiation Imaging (Ministry of Education) and Department of Engineering Physics, Tsinghua University, Beijing 100084, China

1 Introduction

Broad-energy germanium (BEGe) detectors are competitive candidates for neutrinoless double beta decay ($0\nu\beta\beta$) experiments using germanium detectors. Benefiting from the unique electrode structure with a rather small inner electrode for signal output, a BEGe detector performs better than semi-coaxial germanium detectors in energy resolution and pulse shape discrimination (PSD) power for single-site events (SSEs) and multi-site events (MSEs) [1, 2]. This PSD power plays an important role in the background discrimination for $0\nu\beta\beta$ experiments. GERDA (the collaboration of GERmanium Detector Array) used several BEGe detectors for $0\nu\beta\beta$ detection in Phase I and achieved the most sensitive result of all similar experiments using germanium detectors [3]. And to take full advantage of their good performances, much more BEGe detectors are being used in the on-going Phase II of GERDA [4].

During the research of the PSD power of BEGe detectors, fine detector models in both Monte Carlo (MC) simulation and pulse shape simulation (PSS) must be established, so as to evaluate the discrimination efficiency of a developed PSD method and study features of pulse shapes induced by different physical events. In such detector models, the active volume and dead layer thickness are key parameters for obtaining accurate simulation results. Thus, it is necessary to extract specific values of these parameters through characterization of BEGe detectors. GERDA [5–7], and other laboratories [8, 9], have made great efforts in characterization of BEGe detectors, studying the gamma spectrometry performance, the key detector parameters and the pulse shape features.

The $0\nu\beta\beta$ experiments with BEGe detectors will be conducted at China JinPing underground Laboratory (CJPL). As the deepest underground laboratory in the world, CJPL has a rock overburden of 2400 m, or about 6720 m.w.e. (meter water equivalent) [10], and a muon flux of 2.0×10^{-6} m^{-2} s^{-1} [11]. In this work, as the preliminary study of BEGe detectors for $0\nu\beta\beta$ experiments at CJPL, a commercial BEGe detector at CJPL was characterized. Energy resolution and linearity of the detector were investigated, and the efficiencies were calibrated. The detector was scanned with a collimated ^{133}Ba source to measure its active volume, and its dead layer thicknesses on the front and side were measured with an ^{241}Am point source.

2 Experimental

2.1 Detector specification

The detector under investigation is a commercial p-type BEGe detector (Model BE6530) produced by Canberra [12] and has been stored at CJPL for about 4 years. A schematic view of the detector configuration is shown in Fig. 1. The germanium crystal, sized at Φ91.1 mm × 31.4 mm, has a boron-implanted p + electrode of Φ13.5 mm that serves as the signal contact. The lithium-diffused n + electrode covers most of the residual surface of the crystal, serves as the high-voltage contact and is separated from the p + electrode by an annular groove. The crystal is held by a copper cup in a 1.6-mm-thick aluminum endcap and placed 8 mm from the front window. The front window is made of 0.6-mm-thick carbon composite to enhance the detection efficiencies of low-energy gamma rays that penetrate from the front. The recommended bias voltage is +4500 V.

The data acquisition system consists of a charge-sensitive pre-amplifier (Model 2002C), an integrated digital signal analyzer (DSA, Model DSA-LX) and the Genie-2000 software. The pre-amplifier, integrated with the detector, pre-amplifies the charge signal from the p + electrode. The DSA integrates functions of the high-voltage module, main amplifier module and multi-channel analyzer module in an analog electronics chain. It records the signal pulse shapes from the pre-amplifier with a fast sampling ADC (FADC), extracts their energy information through a firmware with the trapezoidal shaping algorithm and finally sends the information to the computer with Genie-2000 software, which addresses the production and storage of energy spectra.

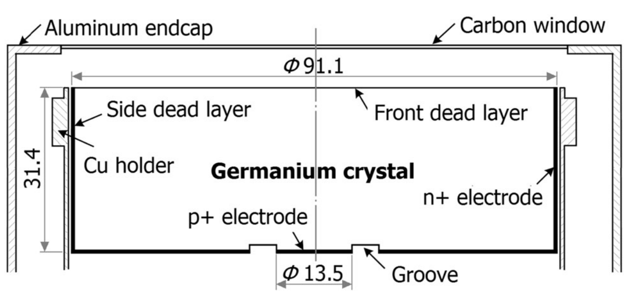

Fig. 1 Schematic view of the BEGe detector

2.2 Experimental procedure

Energy resolution, linearity, efficiencies, active volume size and dead layer thicknesses of the detector were studied.

2.2.1 Energy resolution

Point-like sources of ^{241}Am, ^{133}Ba, ^{137}Cs, ^{60}Co or ^{152}Eu were located approximately 7 cm above top surface of the detector. The point-like sources were of the thin plastic sheet type (Φ32 mm × 4 mm) sealing a dot (Φ1 mm) of the radioactive materials. The ^{60}Co source was measured first to adjust the parameters (rise time and flat top) of the DSA's trapezoidal shaping algorithm. Then, gamma rays of 59.5–1408 keV from the source were measured to obtain energy resolution of the detector.

2.2.2 Linearity

The measured peak locations of corresponding gamma rays were used to check linearity of the detector's response to gamma-ray energy deposition.

2.2.3 Efficiency

The certified cylindrical volume source was obtained in a comparison measurement with National Physical Laboratory, UK. It was a filter medium containing over 10 radioisotopes (^{241}Am, ^{57}Co, ^{60}Co, ^{88}Y, ^{54}Mn, etc.). Absolute detection efficiencies of the detector to the gamma rays were measured by placing the source on the detector. For each γ-ray, the net peak counts were used to deduce the detection efficiency, along with the measurement time, emission intensity of the γ-ray and the source radioactivity.

2.2.4 Active volume size

Gamma rays from the point source of ^{133}Ba were collimated to Φ1 mm × 1 mm with a 1-cm-thick stainless-steel collimator and were used to scan, in steps of 1 or 0.5 cm, the BEGe detector's top and lateral surfaces. The collimator was positioned as close as possible to the endcap surface, in case the enlightened areas in adjacent steps interlap each other. The collimated gamma beams were perpendicular to the detector surfaces. The net peak count at 81 keV was recorded to deduce the active volume.

2.2.5 Dead layer thickness

The ^{241}Am point source was used to measure the front and side dead layer thicknesses. In a certain measurement, the source was placed at a fixed position and the full-energy-peak (FEP) detection efficiency of the 59.5 keV gamma ray was measured (given the certified source activity of $\sim$8290 Bq). Meanwhile, the FEP detection efficiency was also obtained through MC simulation based on GEANT4 with the identical setup as the experiment. The simulation was repeated at different thicknesses of the corresponding dead layer in the detector model; thus, the dependency of FEP detection efficiency on the dead layer thickness was obtained. This dependency relationship was fitted with an exponential function [13], and the real dead layer thickness was determined by interpolating the acquired function to the measured FEP detection efficiency.

2.3 Assembled collimation device

To locate point-like sources at different positions around the detector, an assembled device made of stainless steel was set up to aid the characterization. Figure 2 shows a concept view of the manually operated device. It is composed of three main parts:

a. An L-shaped holder to support all other parts and keep them stable.
b. A position-fixing part to rotate the central shaft and move the source holder, so that point-like sources can be located above the top surface or around the lateral surface of the detector with an error of 1 mm.
c. The removable collimators for the collimated γ-ray beam to scan the detector from different directions.

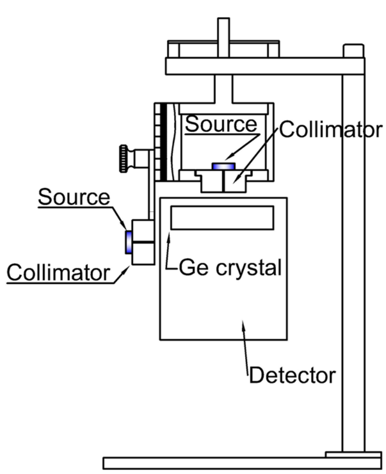

Fig. 2 Concept view of the assembled collimation device for source positioning

Parts (a) and (b) can be disassembled into smaller parts for convenient transportation and storage.

3 Results and discussion

3.1 Energy resolution

For germanium detectors, energy resolutions usually refer to the full width at half maximum (FWHM) of a gamma peak. With a smaller inner signal contact, BEGe detectors can achieve a lower electronics noise level and consequently a better energy resolution than semi-coaxial HPGe detectors [14]. In 0νββ experiments, good energy resolutions are important to narrow the region of interest, distinguish signals from background and improve the experiment sensitivity [15].

Energy resolution of the detector was investigated using ^{60}Co gamma rays (1173 and 1332 keV) first to determine the rise time and flat top of the trapezoidal shaping algorithm of the DSA. By changing the flat top from 0.8 to 1.2 µs at 6 µs of the rise time, the FWHM slightly fluctuated within 0.05 keV (Fig. 3a); while keeping the flat top fixed at 1 µs, the FWHM became better when the rise time was between 2 and 10 µs, fluctuating slightly within 0.06 keV (Fig. 3b). Thus, the flat top at 1 µs and rise time at 6 µs were fixed for subsequent measurements. Based on measurements with the point-like sources, the FWHM was obtained and fitted as a function of the gamma peak energy (E, in keV) by $\mathrm{FWHM} = 0.33\ E^{1/2} + 0.39$, as shown in Fig. 3c, and the FWHM is 1.66 keV ($\sim$0.125 %) at 1.33 MeV, which is outstanding among germanium detectors [16].

3.2 Linearity

Linearity of the responses of germanium detectors to different energy depositions is usually excellent, and the energy calibration data can be well fitted by a linear function. A good linearity leads to a clear discrimination of different physical events based on their energy information.

To study energy response linearity of the BEGe detector, the point-like sources were measured. As the gamma ray of the highest energy is the 1408 keV from ^{152}Eu, the summation peak from the coincidence effect of the ^{60}Co gamma rays was also used to compensate for possible deviation from linearity in high-energy region. As Fig. 4 shows, the detector linearity is notably good.

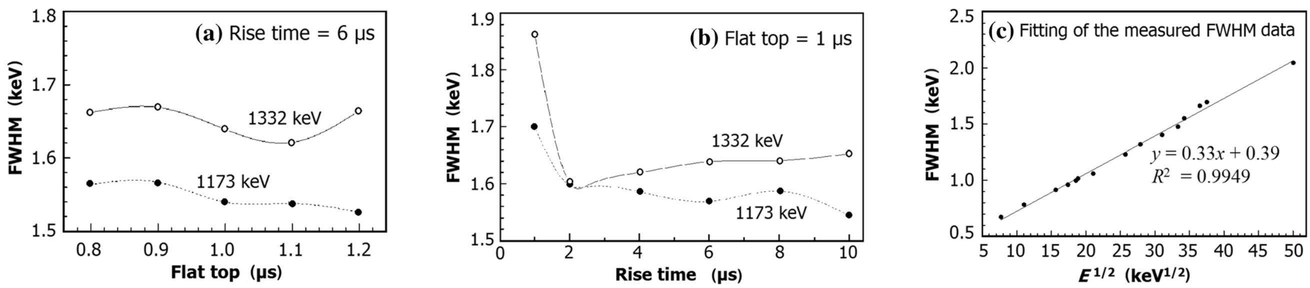

Fig. 3 Energy resolution of the BEGe detector for ^{60}Co γ-rays, versus the flat top (**a**) and rise time (**b**) and the FWHM-$E^{1/2}$ linear fitting (**c**)

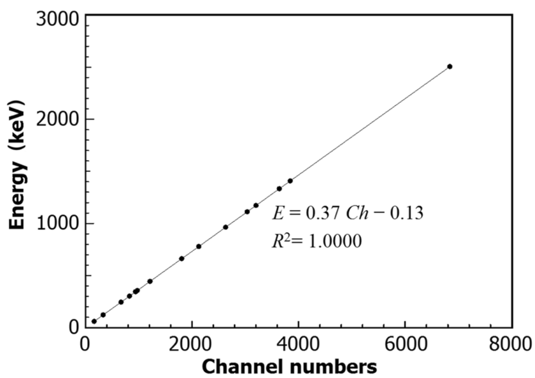

Fig. 4 Linearity of the energy response of the BEGe detector

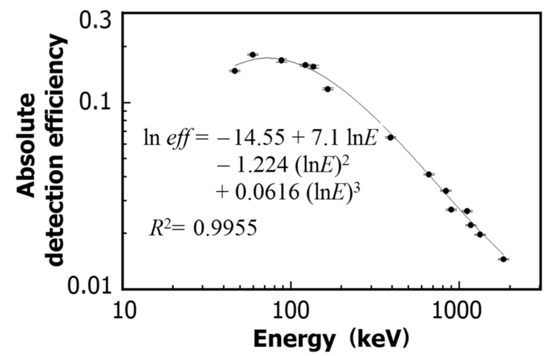

Fig. 5 Absolute detection efficiencies of the BEGe detector. The efficiencies were calibrated using a cylindrical source of multiple gamma rays

3.3 Efficiency

Absolute detection efficiencies of the BEGe detector were measured using the certified cylindrical volume source described in Sect. 2.2, with gamma rays listed in Table 1.

Figure 5 shows the efficiency curve as a function of the gamma-ray energy (in keV), which is fitted by [17]:

$$\ln eff = -14.55 + 7.1 \ln E - 1.224(\ln E)^2 + 0.0616(\ln E)^3,$$

where *eff* is the absolute detection efficiency, and E is the gamma-ray energy. The efficiency reaches its maximum at about 70 keV and decreases almost linearly above 200 keV in double-logarithmic coordinates. Before the maximum point, the probability of the gamma rays to pass through the entrance window and n + electrode of the detector increases with energy; once they succeed in reaching the active volume of the detector, almost all of them are absorbed. After the maximum point, probability of absorbing the gamma photons by the detector decreases with increasing energy.

3.4 Volume scanning

As previously described in Sect. 2.2.4, the measurements were conducted with the collimated ^{133}Ba source, and the net peak count of the 81 keV gamma-ray was used. Figure 6a shows the result along the diameter of the detector, with 0 cm being the surface center. Instead of a curve with flat central plateau and sharp declines at the crystal boundary, the net peak count was maximal at the center, decreased slowly off the center and declined quickly at the boundary. This is attributed to the incomplete collimation of the source. The collimator was 1 cm thick, which was chosen as a result of compromise considering the source of notably low activity (several kBq). A thicker collimator could improve the collimation, but the peak almost disappeared in the background. If the diameter

Table 1 Gamma rays used for the measurement of absolute detection efficiencies

Energy (keV)	46.5	59.5	88.0	122.1	136.5	165.9	391.7	661.7	834.8	898.0	1115.5	1173.2	1332.5	1836.1
Nuclide	^{210}Pb	^{241}Am	^{109}Cd	^{57}Co	^{57}Co	^{139}Ce	^{113}Sn	^{137}Cs	^{54}Mn	^{88}Y	^{65}Zn	^{60}Co	^{60}Co	^{88}Y

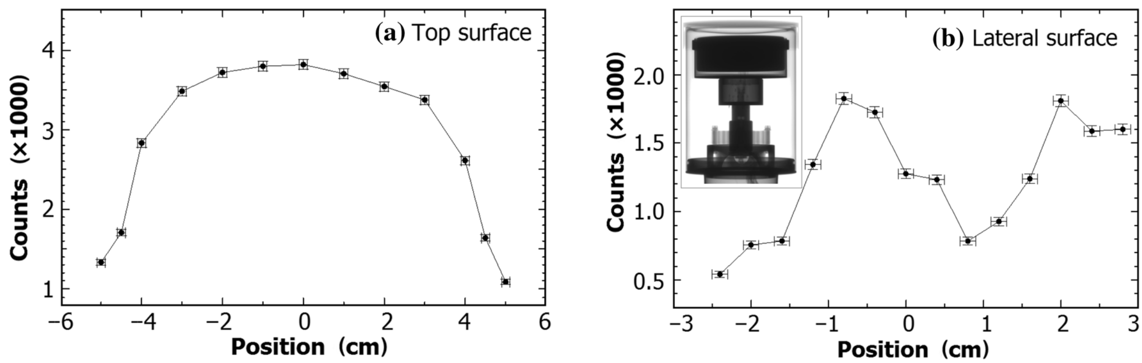

Fig. 6 Net peak counts of the 81 keV peak versus the position of a collimated ^{133}Ba source scanning along the detector's top (**a**) and lateral (**b**) surfaces

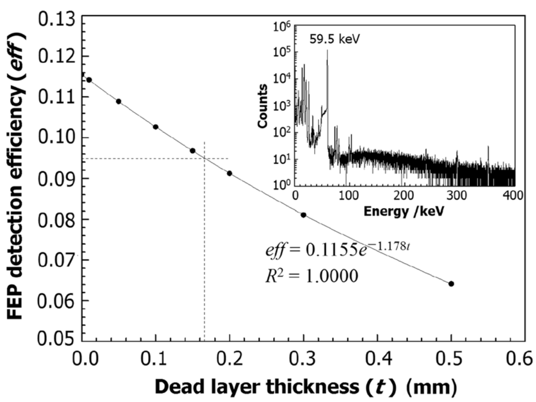

Fig. 7 FEP detection efficiency at 59.5 keV as a function of the front dead layer thickness, obtained from MC simulation. The *dashed lines* indicate the measured efficiency and the corresponding dead layer thickness. The *inset* is spectrum of the ^{241}Am source above the detector

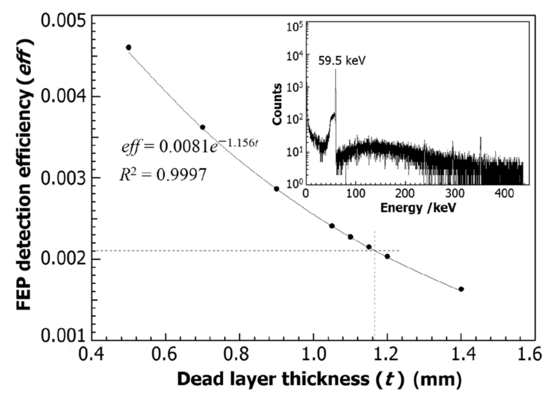

Fig. 8 FEP detection efficiency at 59.5 keV as a function of the side dead layer thickness, obtained from MC simulation. The *dashed lines* indicate the measured efficiency at 0° direction of the ^{241}Am source rotation and the corresponding dead layer thickness. The *inset* is energy spectrum of the ^{241}Am source in the 0° direction

of active volume is defined as the width with the net peak count above 50 % of that at the center, the active volume can be estimated at $\Phi 87.7 \pm 2$ mm, whereas the crystal diameter from the manufacturer is 91.1 mm.

Figure 6b shows the results along the lateral surface, with 0 cm being the same horizontal level as that of the crystal center. The curve does not behave as expected due to the incomplete collimation and the configuration around the crystal. This can be understood by internal structure of the detector, as shown in the inset of Fig. 6b, an X-ray image of the detector. The upper part of the crystal has a thicker copper holder, which absorbed much of the gamma rays when the source moved there, hence the decrease in the net peak counts. When the source moved around the upper boundary of the crystal, the net peak counts increased abnormally because of the increased detection probability of the uncollimated gamma rays passing through the crystal top surface. The net peak counts increased again when the source moved along the lower part of the crystal, where the copper holder was thinner but decreased at the crystal bottom where the copper holder was thicker again. Consequently, it is hard to deduce the thickness of active volume as shown in Fig. 6b, and an improvement with a well-collimated, strong source is necessary.

3.5 Dead layer

Germanium detectors always have dead layers on the surface where electric fields are so weak that electrons and holes cannot be fully collected [17]. Therefore, if a radioactive particle deposits some energy in the dead layers, the total energy recorded by the detector will deviate from the actual energy deposition. For commercial BEGe detectors, typical dead layer thicknesses provided by the manufacturer are merely reference values instead of exclusive ones. Besides, dead layers may grow as time goes by Ref. [18], especially when the detector is stored without applying high voltage for a long time. The ^{241}Am

Table 2 Measurement results of the side dead layer thickness (units: mm)

Nuclides	Gamma rays	0°	45°
^{241}Am	59.5 keV	1.166 ± 0.011	1.192 ± 0.012
^{133}Ba	81 keV/276 keV	1.069 ± 0.029	1.122 ± 0.028
	81 keV/303 keV	1.119 ± 0.021	1.152 ± 0.022
	81 keV/356 keV	1.115 ± 0.017	1.191 ± 0.017
	81 keV/384 keV	1.155 ± 0.028	1.219 ± 0.028

A systematic error of 0.1 mm shall be added to the results

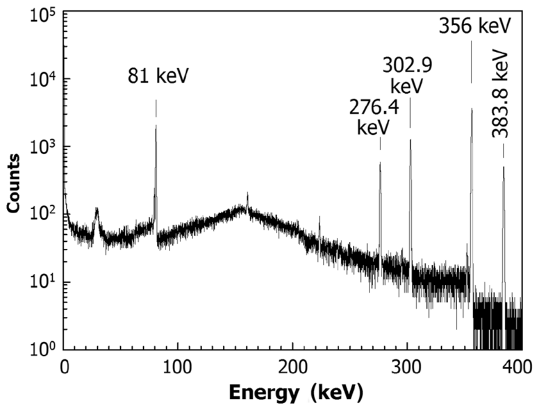

Fig. 9 Energy spectrum of the ^{133}Ba source in the 0° direction

point-like source was used for measuring the dead layer thickness.

The ^{241}Am source was 4 cm above the center of top surface of the detector in measuring the front dead layer thickness (see the inset in Fig. 7 for the energy spectrum). The 59.5 keV peak was fitted by a combined Gaussian and linear function. The net peak count and the FEP detection efficiency were derived based on the fitting result. Figure 7 shows MC simulation results of the FEP detection efficiency as a function of the front dead layer thickness. The data can be fitted by $eff = 0.1155e^{-1.178t}$, and the dashed lines indicate the determined thickness. The final result is 0.166 ± 0.011 (stat) ± 0.1 (syst) mm, whereas the typical value from the manufacturer is 0.3 μm. It is worth mentioning that the standard systematic errors of all results of dead layer thicknesses in Sect. 3.5 were estimated at 0.1 mm, which is a conservative value covering the errors introduced in the processes of source positioning, fitting, simulation, etc.

When the side dead layer thickness was measured, the ^{241}Am source was located at two rotation angles (referred to as the 0° direction and the 45° direction), respectively, on the same horizontal level as the crystal center and 3 cm away from lateral surface of the detector. Similar analyses as that for the top measurement were conducted. The

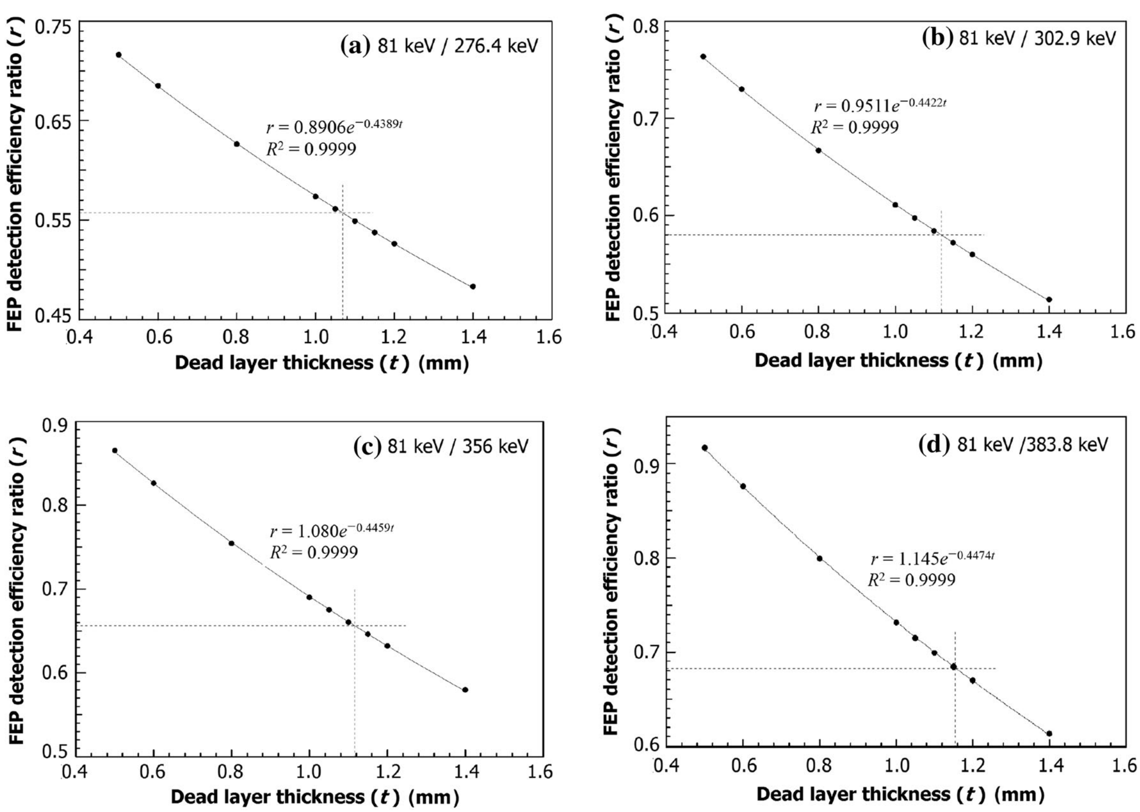

Fig. 10 FEP detection efficiency ratios among gamma rays of ^{133}Ba as a function of the side dead layer thickness, obtained from MC simulation. The *dashed lines* indicate the measured ratios at 0°direction of the source rotation and the corresponding dead layer thicknesses

energy spectrum and the dependency of the FEP detection efficiency on the side dead layer thickness for the 0° direction are shown in Fig. 8, while those for the 45° direction are omitted. The determined dead layer thickness values for both directions are listed in Table 2, which fit well with each other and lead to the average of 1.18 mm, compared to the typical value of 0.5 mm from the manufacturer.

The ^{133}Ba point-like source was also rotated at 0° and 45° to measure the side dead layer thickness, as a benchmark with the ^{241}Am measurements. The whole process was similar to that using ^{241}Am, except that the ratios of the FEP detection efficiencies of the ^{133}Ba gamma rays were obtained in both the experiment and simulation. The FEP detection efficiency ratio between two gamma rays is sensitive to the dead layer thickness, which can be determined by that ratio. Here, the FEP detection efficiency at 81 keV was compared to those at 276, 303, 356 and 384 keV to calculate the ratios. The energy spectrum at 0° direction is shown in Fig. 9, and the dependency of FEP detection efficiency ratios on the side dead layer thickness for the 0° direction is shown in Fig. 10. Those for the 45° direction are omitted. The determined dead layer thickness values from different pairs of gamma rays are also listed in Table 2, which all fit with the results from the ^{241}Am source.

4 Summary

The characterization of a commercial BEGe detector using an assembled collimation device was conducted at CJPL, as the preliminary study for the $0\nu\beta\beta$ experiments in the future. The detector's gamma spectrometry performance is excellent: The energy resolution at 1.33 MeV reaches 1.66 keV, the energy response linearity is perfect and the efficiency curve behaves as expected. The diameter of the active volume is approximately 87.7 mm resulting from the scanning process, whereas a good result of the thickness was not available due to the imperfect experiment conditions. The front and side dead layer thicknesses are approximately 0.17 and 1.18 mm, respectively, which have increased compared to the typical values from the manufacturer. The determined dead layer thickness values will be applied to the detector models for MC simulation and PSS, whereas the active volume size will be further measured using a strong source with good collimation.

The pulse shapes of the BEGe detector are to be studied. A systematic pulse shape analysis method will be established for BEGe detectors, which will contribute to the background discrimination in the prospective $0\nu\beta\beta$ experiments at CJPL.

References

1. A. di Vacri, M. Agostini, E. Bellotti, et al. (2009) Characterization of broad energy germanium detector as a candidate for the GERDA experiment, in the 2009 IEEE Nuclear Science Symposium and Medical Imaging Conference (NSS/MIC), Orlando, USA, Oct. 25–31, pp. 1761–1767
2. D. Budjáš, M.B. Heider, O. Chkvorets et al., Pulse shape discrimination studies with a broad-energy Germanium detector for signal identification and background suppression in the GERDA double beta decay experiment. J. Instrum. **4**(10), P10007 (2009). doi:10.1088/1748-0221/4/10/P10007
3. M. Agostini, M. Allardt, E. Andreotti et al., Results on neutrinoless double-β decay of ^{76}Ge from Phase I of the GERDA experiment. Phys. Rev. Lett. **111**, 122503 (2013). doi:10.1103/PhysRevLett.111.122503
4. V. D'Andrea. Status Report of the GERDA Phase II Startup. arXiv preprint arXiv:1604.05016
5. M. Agostini, E. Bellotti, R. Brugnera et al., Characterization of a broad energy germanium detector and application to neutrinoless double beta decay search in 76 Ge. J. Instrum. **6**(04), P4005 (2011). doi:10.1088/1748-0221/6/04/P04005
6. E. Andreotti, Characterization of BEGe detectors in the HADES underground laboratory. Nucl. Instru. Methods Phys. Res. A **718**, 475–477 (2013). doi:10.1016/j.nima.2012.11.053
7. M. Agostini, M. Allardt, E. Andreotti et al., Production, characterization and operation of ^{76}Ge enriched BEGe detectors in GERDA. Eur. Phys. J. C **75**(2), 1–22 (2014). doi:10.1140/epjc/s10052-014-3253-0
8. D. Barrientos, A.J. Boston, H.C. Boston et al., Characterisation of a Broad Energy Germanium (BEGe) detector. Nucl. Instru. Methods Phys. Res. A **648**, S228–S231 (2011). doi:10.1016/j.nima.2010.11.129
9. L.J. Harkness-Brennan, D.S. Judson, A.J. Boston et al., An experimental characterisation of a Broad Energy Germanium detector. Nucl. Instru. Methods A **760**, 28–39 (2014). doi:10.1016/j.nima.2014.05.080
10. K.J. Kang, J.P. Cheng, Y.H. Chen et al., Status and prospects of a deep underground laboratory in China. J. Phys Conf. Ser. **203**(1), 12028 (2010). doi:10.1088/1742-6596/203/1/012028
11. Y.C. Wu, X.Q. Hao, Q. Yue et al., Measurement of cosmic ray flux in the China JinPing underground laboratory. Chin. Phys. C **37**(8), 086001 (2013). doi:10.1088/1674-1137/37/8/086001
12. CANBERRA Industries Inc., http://www.canberra.com/
13. D. Budjáš, M. Heisel, W. Maneschg et al., Optimisation of the MC-model of a p-type Ge-spectrometer for the purpose of efficiency determination. Appl. Radiat. Isot. **67**(5), 706–710 (2009). doi:10.1016/j.apradiso.2009.01.015
14. P.S. Barbeau, J.I. Collar, O. Tench, Large-mass ultralow noise germanium detectors: performance and applications in neutrino and astroparticle physics. J. Cosmol. Astropart. Phys. **2007**(09), 9 (2007). doi:10.1088/1475-7516/2007/09/009
15. B. Schwingenheuer, Status and prospects of searches for neutrinoless double beta decay. Ann. Phys. **525**(4), 269–280 (2013). doi:10.1002/andp.201200222
16. G. Gilmore, *Practical Gamma-ray spectrometry*, 2nd edn. (Wiley, Hoboken, 2008), pp. 138–141
17. G.F. Knoll, *Radiation detection and measurement* (Wiley, Hoboken, 2010), pp. 423–424
18. N.Q. Huy, The influence of dead layer thickness increase on efficiency decrease for a coaxial HPGe p-type detector[J]. Nucl. Instru. Methods A **621**(1), 390–394 (2010). doi:10.1016/j.nima.2010.05.007